

New Developments Of Cutting Theories With Respect To Dredging. The Cutting Of Clay.

Dr.ir. S.A. Miedema

Abstract.
Introduction, the Rate Process Theory.
Proposed Rate Process Theory.
Comparison of Proposed Theory with some other Theories.
Verification of the Theory Developed.
The Cutting of Clay.
Discussion and Conclusions.
Acknowledgements.
Bibliography.
Software used.
List of Symbols used.

Abstract.

From literature on this subject it is known that the process of cutting clay is different from that of water saturated sand. Sand is often modeled as a continuum with an internal friction angle and a sand/steel friction angle but without cohesion and adhesion. Clay is considered to be a continuum with cohesion and adhesion, but with an internal friction angle and a clay/steel friction angle equal to zero. In this paper clay will be considered this way. It has been noticed by many researchers that the cohesion and adhesion of clay increase with an increasing deformation rate. It has also been noticed that the failure mechanism of clay can be of the "flow type" or the "tear type", similar to the mechanisms that occur in steel cutting. Previous researchers, especially Mitchell 1976 [5], have derived equations for the strain rate dependency of the cohesion based on the "rate process theory".

However the resulting equations did not allow pure cohesion and adhesion. In many cases the equations derived resulted in a yield stress of zero or minus infinity for a material at rest. Also empirical equations have been derived giving the same problems.

Based on the "rate process theory" with an adapted Boltzman probability distribution, the Mohr-Coulomb failure criteria will be derived in a form containing the influence of the deformation rate on the parameters involved. The equation derived allows a yield stress for a material at rest and does not contradict the existing equations, but confirms measurements of previous researchers. The equation derived can be used for silt and for clay, giving both materials the same physical background.

Based on the equilibrium of forces on the chip of soil cut, as derived by Miedema 1987 [4] for soil in general, criteria are formulated to predict the failure mechanism when cutting clay. A third failure mechanism can be distinguished, the "curling type". Combining the equation for the deformation rate dependency of cohesion and adhesion with the derived cutting equations, allows the prediction of the failure mechanism and the cutting forces involved. The theory developed has been verified by using data obtained by Hatamura and Chijiwa 1975-1977 [2] with respect to the adapted rate process theory and data obtained by Stam 1983 [8] with respect to the cutting forces. However since the theory developed confirms the work carried out by previous researchers its validity has been proven in advance. In this paper simplifications have been applied to allow a clear description of the phenomena involved.

Introduction, the Rate Process Theory.

It has been noticed by many researchers that the cohesion and adhesion of clay increase with an increasing deformation rate. It has also been noticed that the failure mechanism of clay can be of the "flow type" or the "tear type", similar to the mechanisms that occur in steel cutting.

The rate process theory can be used to describe the phenomena occurring in the processes involved. This theory, developed by Glasstone, Laidler and Eyring 1941 [1] for the modeling of absolute reaction rates, has been made applicable to soil mechanics by Mitchell 1976 [5].

Although there is no physical evidence of the validity of this theory it has proved valuable for the modeling of many processes such as chemical reactions.

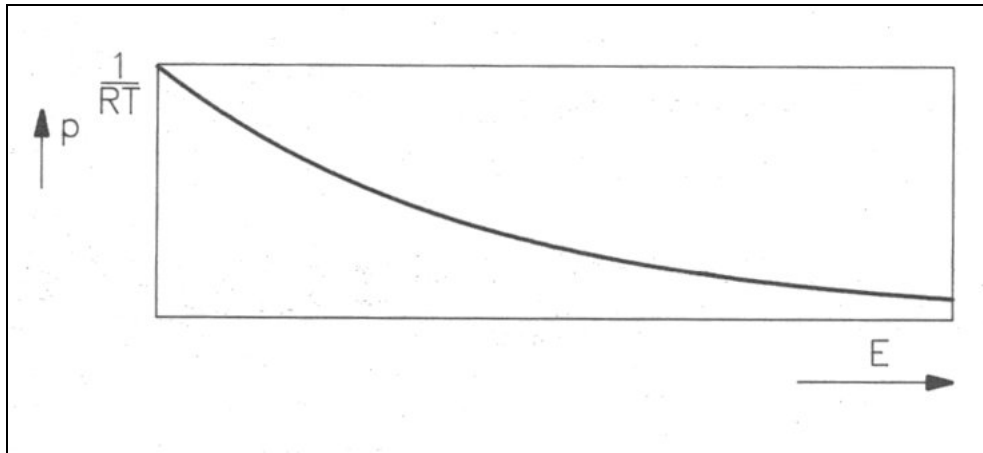


Fig. 1: The Boltzmann probability distribution.

The rate process theory, however, does not allow strain rate independent stresses such as real cohesion and adhesion. This connects with the starting point of the rate process theory that the probability of atoms, molecules or particles, termed flow units having a certain thermal vibration energy is in accordance with the Boltzmann distribution (fig. 1):

$$p(E) = \frac{1}{R \cdot T} \cdot \exp \left[\frac{-E}{R \cdot T} \right] \quad (1)$$

The movement of flow units participating in a time dependent flow is constrained by energy barriers separating adjacent equilibrium positions. To

cross such an energy barrier, a flow unit should have an energy level exceeding a certain activation energy E_a .

The probability of a flow unit having an energy level greater than a certain energy level E_a can be calculated by integrating the Boltzmann distribution from the energy level E_a to infinity, as depicted in figure 2, this gives:

$$P_{E>E_a} = \exp\left[\frac{-E_a}{R \cdot T}\right] \quad (2)$$

The value of the activation energy E_a depends on the type of material and the process involved. Since thermal vibrations occur at a frequency given by kT/h , the frequency of activation of crossing energy barriers is:

$$\nu = \frac{k \cdot T}{h} \cdot \exp\left[\frac{-E_a}{R \cdot T}\right] \quad (3)$$

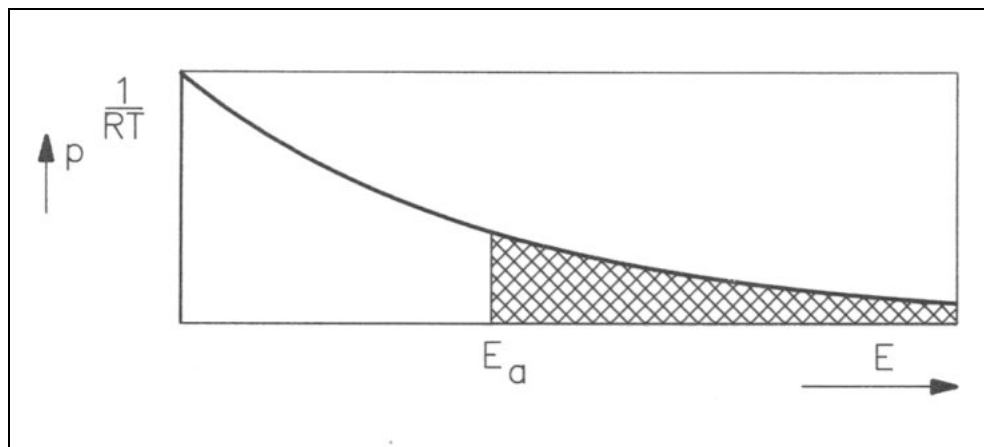


Fig. 2: The probability of exceeding an energy level E_a .

In a material at rest the barriers are crossed with equal frequency in all directions. If however a material is subjected to an external force resulting in directional potentials on the flow units, the barrier height in the direction of the force is reduced by $(f \cdot \lambda / 2)$ and raised by the same amount in the opposite direction. Where f represents the force acting on a flow unit and λ represents the distance between two successive equilibrium positions. From this it can be

derived that the net frequency of activation in the direction of the force f is as illustrated in figure 3:

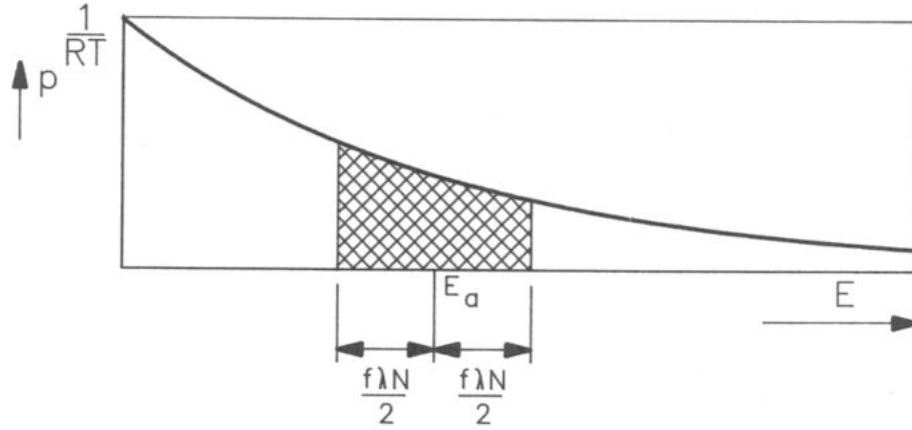


Fig. 3: The probability of net activation in direction of force.

$$v = \frac{k \cdot T}{h} \cdot \exp \left[\frac{-E_a}{R \cdot T} \right] \cdot \left\{ \exp \left[\frac{+f \cdot \lambda}{2 \cdot k \cdot T} \right] - \exp \left[\frac{-f \cdot \lambda}{2 \cdot k \cdot T} \right] \right\} \quad (4)$$

If a shear stress τ is distributed uniformly along S bonds between flow units per unit area then $f = \tau/S$ and if the strain rate is a function X of the proportion of successful barrier crossings and the displacement per crossing according to $d\epsilon/dt = X \cdot v$ then:

$$\dot{\epsilon} = 2 \cdot X \cdot \frac{k \cdot T}{h} \cdot \exp \left[\frac{-E_a}{R \cdot T} \right] \cdot \sinh \left[\frac{\tau \cdot \lambda \cdot N}{2 \cdot S \cdot R \cdot T} \right] \quad \text{with: } R = N \cdot k \quad (5)$$

From this equation, simplified equations can be derived to obtain dashpot coefficients for rheological models, to obtain functional forms for the influences of different factors on strength and deformation rate, and to study deformation mechanisms in soils. For example:

$$\text{if } \left[\frac{\tau \cdot \lambda \cdot N}{2 \cdot S \cdot R \cdot T} \right] < 1 \quad \text{then } \sinh \left[\frac{\tau \cdot \lambda \cdot N}{2 \cdot S \cdot R \cdot T} \right] \approx \left[\frac{\tau \cdot \lambda \cdot N}{2 \cdot S \cdot R \cdot T} \right] \quad (6)$$

resulting in the mathematical description of a Newtonian fluid flow, and:

$$\text{if } \left[\frac{\tau \cdot \lambda \cdot N}{2 \cdot S \cdot R \cdot T} \right] > 1 \quad \text{then} \quad \sinh \left[\frac{\tau \cdot \lambda \cdot N}{2 \cdot S \cdot R \cdot T} \right] \approx \frac{1}{2} \cdot \exp \left[\frac{\tau \cdot \lambda \cdot N}{2 \cdot S \cdot R \cdot T} \right] \quad (7)$$

resulting in a description of the Mohr-Coulomb failure criterium for soils as proposed by Mitchel [5] in 1968. Yao and Zeng 1991 [12, 13] used the first simplification (6) to derive a relation between soil shear strength and shear rate and the second simplification (7) to derive a relation between soil-metal friction and sliding speed.

Proposed Rate Process Theory.

The rate process theory does not allow for shear strength if the deformation rate is zero. This implies that creep will always occur since any material is always exposed to its own weight. This results from the starting point of the rate process theory, the Boltzman distribution of the probability of a flow unit exceeding a certain energy level of thermal vibration.

According to the Boltzman distribution there is always a probability that a flow unit exceeds an energy level, between an energy level of zero and infinity, this is illustrated in figure 2.

Since the probability of a flow unit having an infinite energy level is infinitely small, the time-span between the occurrence of flow units having an infinite energy level is also infinite, if a finite number of flow units is considered. From this it can be deduced that the probability that the energy level of a finite number of flow units does not exceed a certain limiting energy level in a finite time-span is close to 1. This validates the assumption that for a finite number of flow units in a finite time-span the energy level of a flow unit cannot exceed a certain limiting energy level E_l . The resulting adapted Boltzman distribution is illustrated in figure 4. The Boltzman distribution might be a good approximation for atoms and molecules but for particles consisting of many atoms and/or molecules the distribution according to figure 4 seems more reasonable, since it has never been noticed that sand grains in a layer of sand at rest, start moving because of their internal energy. In clay some movement of the clay particles seems probable since the clay particles are much smaller than the sand particles. Since particles consist of many atoms, the net vibration energy in any direction will be small, because the atoms vibrate thermally with equal frequency in all directions.

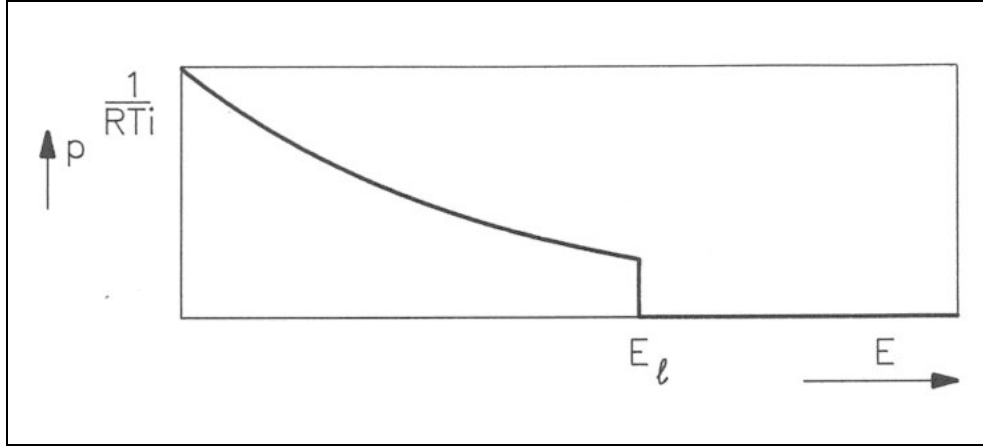


Fig. 4: The adapted Boltzman probability distribution.

If a probability distribution according to figure 4 is considered, the probability of a particle exceeding a certain activation energy E_a becomes:

$$P_{E>E_a} = \frac{\exp\left[\frac{-E_a}{R \cdot T}\right] - \exp\left[\frac{-E_l}{R \cdot T}\right]}{1 - \exp\left[\frac{-E_l}{R \cdot T}\right]} \quad \text{if } E_a < E_l \quad (8)$$

and

$$P_{E>E_a} = 0 \quad \text{if } E_a > E_l \quad (9)$$

If the material is now subjected to an external shear stress, four cases can be distinguished with respect to the strain rate.

Case 1: The energy level $E_a + \tau\lambda N/2S$ is smaller then the limiting energy level E_l (figure 5). The strain rate equation is now:

$$\dot{\epsilon} = 2 \cdot X \cdot \frac{k \cdot T}{h \cdot i} \cdot \exp\left[\frac{-E_a}{R \cdot T}\right] \cdot \sinh\left[\frac{\tau \cdot \lambda \cdot N}{2 \cdot S \cdot R \cdot T}\right] \quad (10)$$

With: $i = 1 - \exp\left[\frac{-E_l}{R \cdot T}\right]$

Except for the coefficient i , necessary to ensure that the total probability remains 1, equation (10) is identical to equation (5).

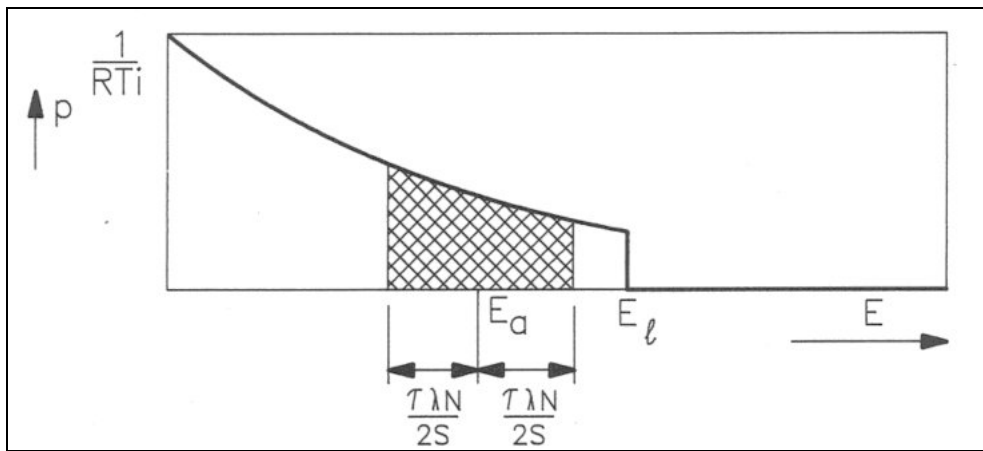


Fig. 5: The probability of net activation in case 1.

Case 2: The activation energy E_a is less than the limiting energy E_l , but the energy level $E + \tau\lambda N/2S$ is greater than the limiting energy level E_l (figure 6).

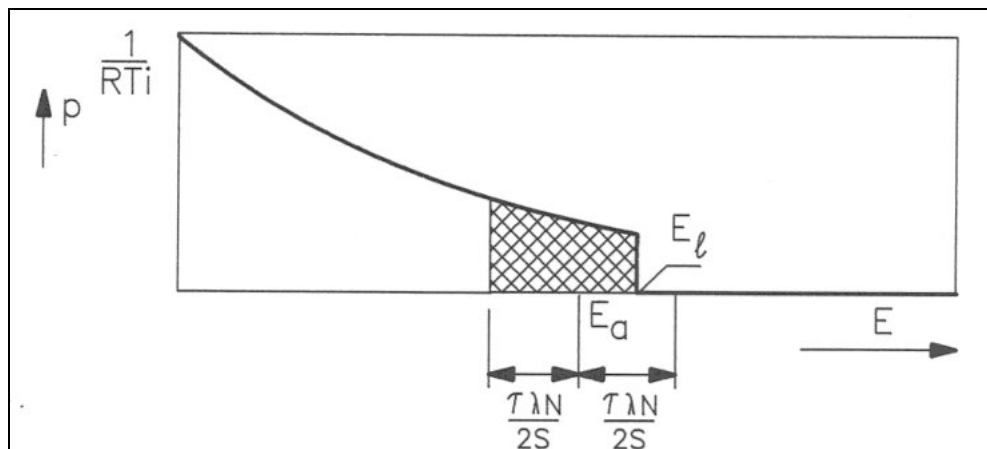


Fig. 6: The probability of net activation in case 2.

The strain rate equation is now:

$$\dot{\epsilon} = X \cdot \frac{k \cdot T}{h \cdot i} \cdot \left\{ \exp \left[- \left(\frac{E_a}{R \cdot T} - \frac{\tau \cdot \lambda \cdot N}{2 \cdot S \cdot R \cdot T} \right) \right] - \exp \left[\frac{-E_l}{R \cdot T} \right] \right\} \quad (11)$$

Case 3: The activation energy E_a is greater than the limiting energy E_l , but the energy level $E_a - \tau\lambda N/2S$ is less than the limiting energy level E_l (figure 7). The strain rate equation is now:

$$\dot{\epsilon} = X \cdot \frac{k \cdot T}{h \cdot i} \cdot \left\{ \exp \left[- \left(\frac{E_a}{R \cdot T} - \frac{\tau \cdot \lambda \cdot N}{2 \cdot S \cdot R \cdot T} \right) \right] - \exp \left[\frac{-E_l}{R \cdot T} \right] \right\} \quad (12)$$

Equation (12) appears to be identical to equation (11), but the boundary conditions differ.

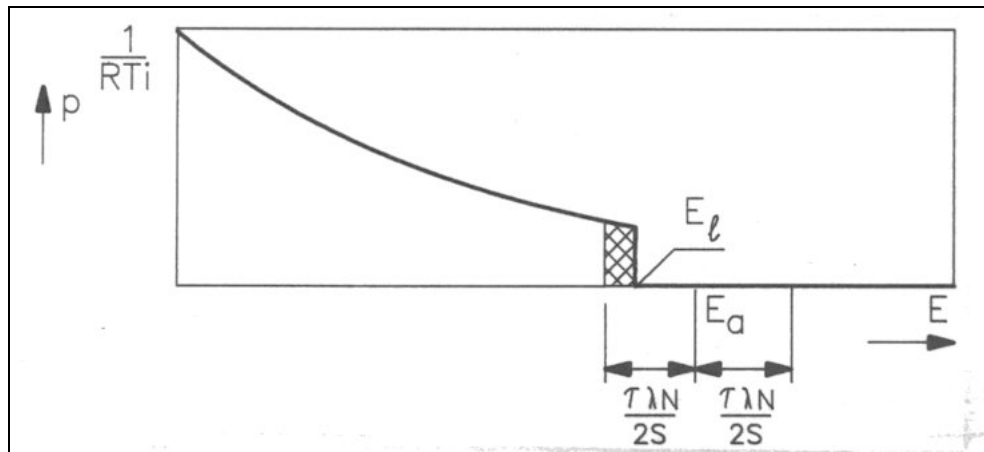


Fig. 7: The probability of net activation in case 3.

Case 4: The activation energy E_a is greater than the limiting energy E_l and the energy level $E_a - \tau\lambda N/2S$ is greater than the limiting energy level E_l (figure 8). The strain rate will be equal to zero in this case.

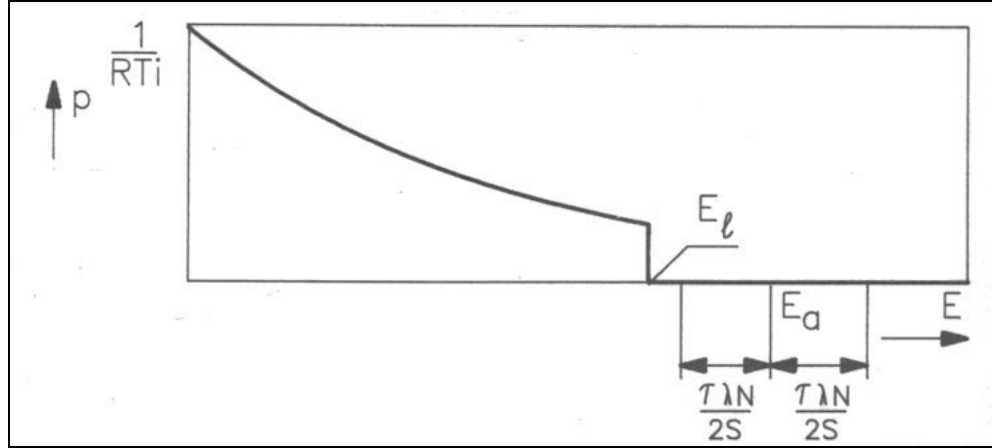


Fig. 8: The probability of net activation in case 4.

The cases 1 and 2 are similar to the case considered by Mitchell 1976 [5] and still do not permit true cohesion and adhesion. Case 4 considers particles at rest without changing position within the particle matrix. Case 3 considers a material on which an external shear stress of certain magnitude must be applied to allow the particles to cross energy barriers, resulting in a yield stress (true cohesion or adhesion). From equation (12) the following equation for the shear stress can be derived:

$$\tau = (E_a - E_l) \cdot \frac{2 \cdot S}{\lambda \cdot N} + R \cdot T \cdot \frac{2 \cdot S}{\lambda \cdot N} \cdot \ln \left[1 + \frac{\dot{\epsilon}}{\dot{\epsilon}_0} \right] \quad (13)$$

$$\text{With: } \dot{\epsilon}_0 = \frac{X \cdot k \cdot T}{h \cdot i} \cdot \exp \left[\frac{-E_l}{R \cdot T} \right]$$

According to Mitchell 1976 [5], if no shattering of particles occurs, the relation between the number of bonds S and the effective stress σ_e can be described by the following equation:

$$S = a + b \cdot \sigma_e \quad (14)$$

Lobanov and Joanknecht 1980 [3] confirmed this relation implicitly for pressures up to 10 bar for clay and paraffin wax. At very high pressures they

found an exponential relation which might be caused by internal failure of the particles. For the friction between soil and metal Yao and Zeng 1988 [13] also used equation (14), but for the internal friction Yao and Zeng 1991 [12] used a logarithmic relationship which contradicts Lobanov and Joanknecht and Mitchell, although it can be shown by Taylor series approximation that a logarithmic relation can be transformed into a linear relation for values of the argument of the logarithm close to 1. Since equation (14) contains the effective stress it is necessary that the clay used is fully consolidated. Substituting equation (14) in equation (13) gives:

$$\tau = a \cdot \left\{ (E_a - E_\ell) \cdot \frac{2}{\lambda \cdot N} + R \cdot T \cdot \frac{2}{\lambda \cdot N} \cdot \ln \left[1 + \frac{\dot{\epsilon}}{\dot{\epsilon}_0} \right] \right\} + b \cdot \left\{ (E_a - E_\ell) \cdot \frac{2}{\lambda \cdot N} + R \cdot T \cdot \frac{2}{\lambda \cdot N} \cdot \ln \left[1 + \frac{\dot{\epsilon}}{\dot{\epsilon}_0} \right] \right\} \cdot \sigma_e \quad (15)$$

Equation (15) is of the same form as the Mohr-Coulomb failure criterium:

$$\tau = \tau_c + \sigma_e \cdot \tan(\phi) \quad (16)$$

Equation (15), however, allows the strain rate to become zero, which is not possible in the equation derived by Mitchell 1976 [5]. The Mitchell equation and also the equations derived by Yao and Zeng 1988-1991 [12, 13] will result in a negative shear strength at small strain rates.

Comparison of Proposed Theory with some other Theories.

The proposed new theory is in essence similar to the theory developed by Mitchell 1976 [5] which was based on the "rate process theory" as proposed by Eyring 1941 [1]. It was no, however, necessary to use simplifications to obtain the equation in a useful form. The following formulation for the shear stress as a function of the strain rate has been derived by Mitchell by simplification of equation (5):

$$\tau = a \cdot \left\{ \frac{E_a}{\lambda \cdot N} + R \cdot T \cdot \frac{2}{\lambda \cdot N} \cdot \ln \left[\frac{\dot{\epsilon}}{B} \right] \right\} + b \cdot \left\{ \frac{E_a}{\lambda \cdot N} + R \cdot T \cdot \frac{2}{\lambda \cdot N} \cdot \ln \left[\frac{\dot{\epsilon}}{B} \right] \right\} \cdot \sigma_e \quad (17)$$

$$\text{With: } B = \frac{X \cdot k \cdot T}{h}$$

This equation is not valid for very small strain rates, because this would result in a negative shear stress. It should be noted that for very high strain rates the equations (15) and (17) will have exactly the same form.

Zeng and Yao 1991 [12] derived the following equation by simplification of equation (5) and by adding some empirical elements:

$$\ln(\tau) = C_1 + C_2 \cdot \ln(\dot{\epsilon}) + C_3 \cdot \ln(1 + C_4 \cdot \sigma_e) \quad (18)$$

Rewriting equation (18) in a more explicit form gives:

$$\tau = \exp[C_1] \cdot (\dot{\epsilon})^{C_2} \cdot (1 + C_4 \cdot \sigma_e)^{C_3} \quad (19)$$

Equation (19) is valid for strain rates down to zero, but not for a yield stress. With respect to the strain rate, equation (19) is the equation of a fluid behaving according to the power law named "power law fluids". It should be noted however that equation (19) cannot be derived from equation (5) directly and thus should be considered as an empirical equation. If the coefficient C_3 equals 1, the relation between shear stress and effective stress is similar to the relation found by Mitchell 1976 [5].

For the friction between the soil (clay and loam) and metal Yao and Zeng 1988 [13] derived the following equation by simplification of equation (5):

$$\tau_b = \tau_{ya} + C_5 \cdot \ln[\dot{\epsilon}] + \sigma_e \cdot \tan[\delta] = \tau_a + \sigma_e \cdot \tan[\delta] \quad (20)$$

Equation (20) allows a yield stress, but does not allow the sliding velocity to become zero. An important conclusion of Yao and Zeng is that pasting soil on the metal surface slightly increases the friction meaning that the friction between soil and metal almost equals the shear strength of the soil.

The above mentioned researchers based their theories on the rate process theory, other researchers derived empirical equations.

Turnage and Freitag 1970 [9] observed that for saturated clays the cone resistance varied with the penetration rate according to:

$$F = a \cdot v^b \quad (21)$$

With values for the exponent ranging from 0.091 to 0.109. Wismer and Luth 1972 [10] confirmed this relation and found a value of 0.100 for the exponent, not only for cone penetration tests but also for the relation between the cutting forces and the cutting velocity when cutting clay with straight blades. Hatamura and Chijiwa 1975-1977 [2] also confirmed this relation for clay and loam cutting and found an exponent of 0.089.

Soydemir 1977 [7] derived an equation similar to the Mitchell equation. From the data measured by Soydemir a relation according to equation (21) with an exponent of 0.101 can be derived. This confirms both the Mitchell approach and the power law approach.

Verification of the Theory Developed.

The theory developed differs from the other theories mentioned in the previous paragraph, because the resulting equation (15) allows a yield strength (cohesion or adhesion). At a certain consolidation pressure level equation (15) can be simplified to:

$$\tau = \tau_y + \tau_0 \cdot \ln \left[1 + \frac{\dot{\epsilon}}{\dot{\epsilon}_0} \right] \quad (22)$$

If $(d\epsilon/dt)/(d\epsilon_0/dt) \ll 1$, equation (22) can be approximated by:

$$\tau = \tau_y + \tau_0 \cdot \frac{\dot{\epsilon}}{\dot{\epsilon}_0} \quad (23)$$

This approximation gives the formulation of a Bingham fluid. If the yield strength τ_y is zero, equation (23) represents a Newtonian fluid.

If $(d\varepsilon/dt)/(d\varepsilon_0/dt) \gg 1$, equation (22) can be approximated by:

$$\tau = \tau_y + \tau_0 \cdot \ln \left[\frac{\dot{\varepsilon}}{\dot{\varepsilon}_0} \right] \quad (24)$$

This approximation is similar to equation (17) as derived by Mitchell.

If $(d\varepsilon/dt)/(d\varepsilon_0/dt) \gg 1$ and $\tau - \tau_y \ll \tau_y$, equation (22) can be approximated by:

$$\tau = \tau_y \cdot \left[\frac{\dot{\varepsilon}}{\dot{\varepsilon}_0} \right]^{\tau_0/\tau_y} \quad (25)$$

This approximation is similar to equation (21) as found empirically by Wismer and Luth 1972 [10] and many other researchers. The equation (15) derived in this paper, the equation (17) derived by Mitchell and the empirical equation (21) as used by many researchers have been fitted to data obtained by Hatamura and Chijiiwa 1975-1977 [2]. This is illustrated in figure 9 with a logarithmic horizontal axis. Figure 10 gives an illustration with both axis logarithmic. These figures show that the data obtained by Hatamura and Chijiiwa fit well and that the above described approximations are valid. The values used are $\tau_y = 28$ kPa, $\tau_0 = 4$ kPa and $\varepsilon_0 = 0.03$ /s.

It is assumed that adhesion and cohesion can both be modelled according to equation (22). The research carried out by Yao and Zeng 1988 [13] validates the assumption that this is true for adhesion.

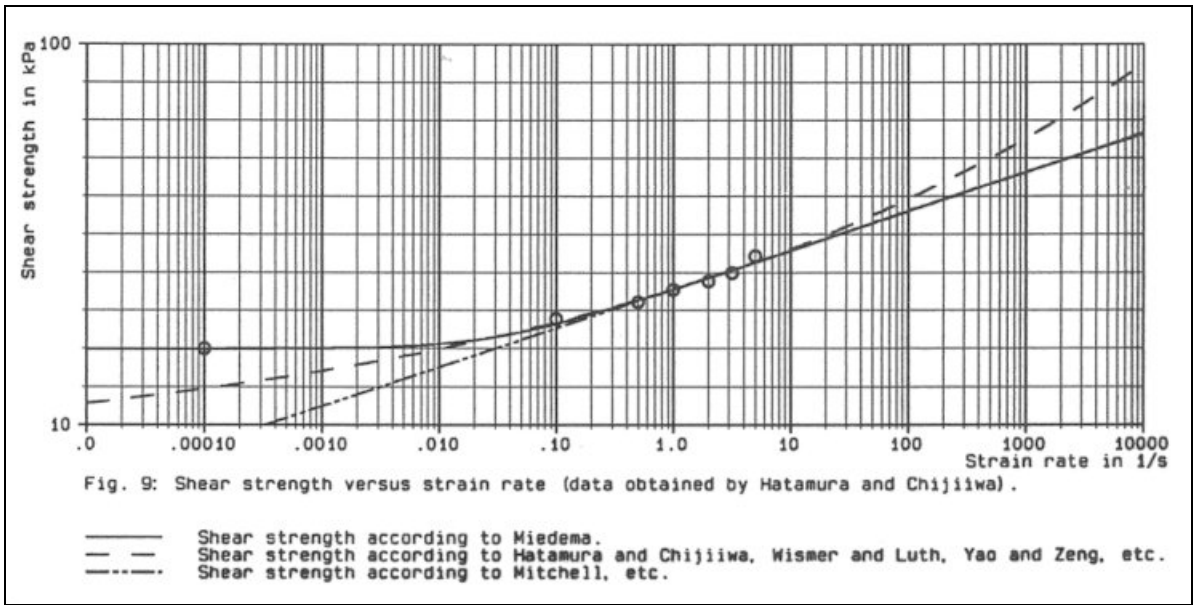


Fig. 9: Shear stress as a function of strain rate with the horizontal axis logarithmic.

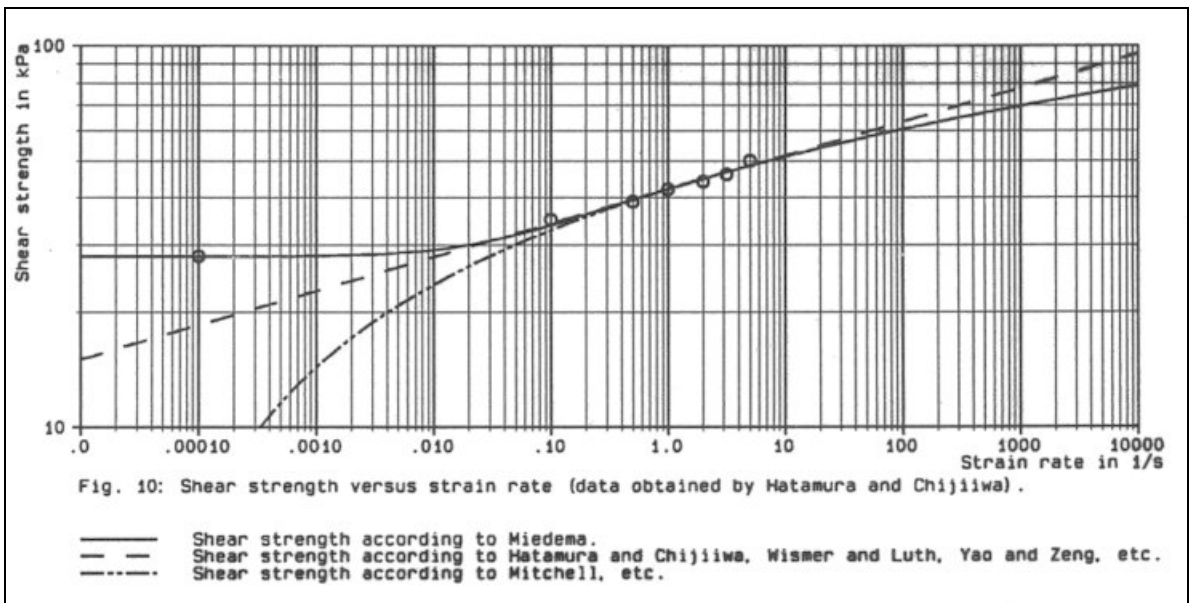


Fig. 10: Shear stress as a function of strain rate with logarithmic axis.

The Cutting of Clay.

In 1975 Hatamura and Chijiwa [2] distinguished three failure mechanisms in soil cutting. The "shear type", the "flow type" and the "tear type". The "shear type" occurs in materials with an angle of internal friction like sand and will be

left out of order. A fourth failure mechanism can be distinguished, the "curling type", as is known in metal cutting. Although it seems that the curling of the chip cut is part of the flow of the material, whether the "curling type" or the "flow type" occurs depends on several conditions.

Figure 16 illustrates the three failure mechanism as they might occur when cutting clay. To predict which type of failure mechanism will occur under given conditions with a specific clay, a formulation for the cutting forces has to be derived. The derivation is made under the assumption that the stresses on the shear plane and the blade are constant and equal to the average stresses acting on the surfaces.

The forces acting on a straight blade when cutting soil, can be differentiated as:

1. A force normal to the blade N_2 .
2. A shear force S_2 as a result of the soil/steel friction $N_2 \cdot \tan[\delta]$.
3. A shear force A as a result of pure adhesion between the soil and the blade τ_a . This force can be calculated by multiplying the adhesive shear strength τ_a of the soil with the contact area between the soil and the blade.
4. A force W_2 as a result of water under pressure on the blade.

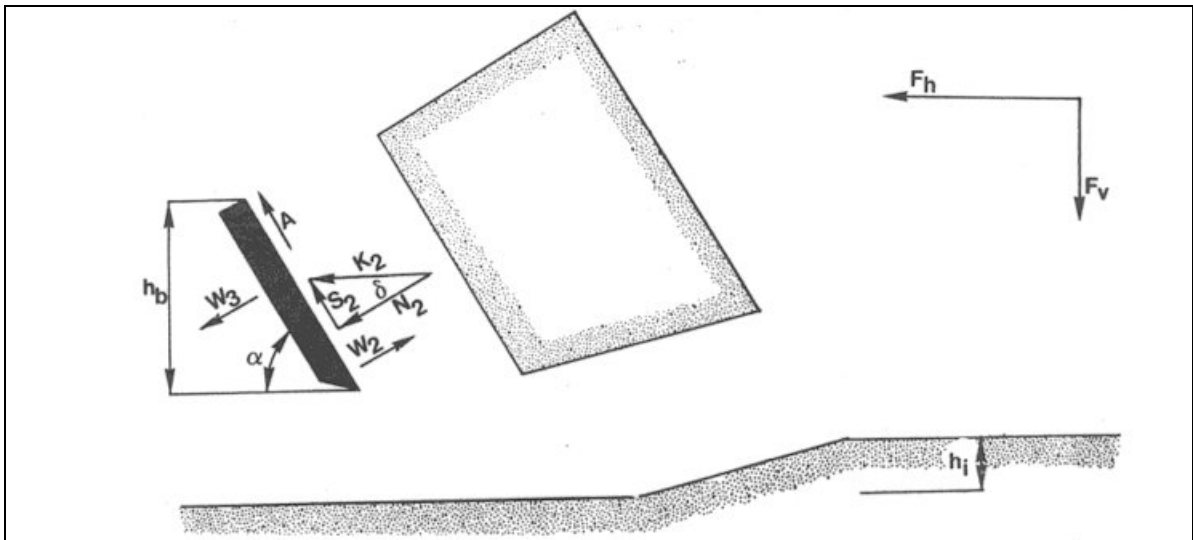


Fig. 11: The forces acting on the blade.

These forces are shown in figure 11. If the forces N_2 and S_2 are combined to a resulting force K_2 and the adhesive force and the water under pressures are known, then the resulting force K_2 is the unknown force on the blade.

Figure 12 illustrates the forces on the layer of soil cut. The forces shown are valid in general. In clay several forces can be neglected.

The forces acting on this layer are:

1. The forces occurring on the blade as mentioned above.
2. A normal force acting on the shear surface N_1 .
3. A shear force S_1 as a result of internal friction $N_1 \cdot \tan[\phi]$.
4. A force W_1 as a result of water under pressure in the shear zone.
5. A shear force C as a result of pure cohesion τ_c . This force can be calculated by multiplying the cohesive shear strength τ_c with the area of the shear plane.
6. A gravity force G as a result of the weight of the layer cut.
7. An inertial force I , resulting from acceleration of the soil.

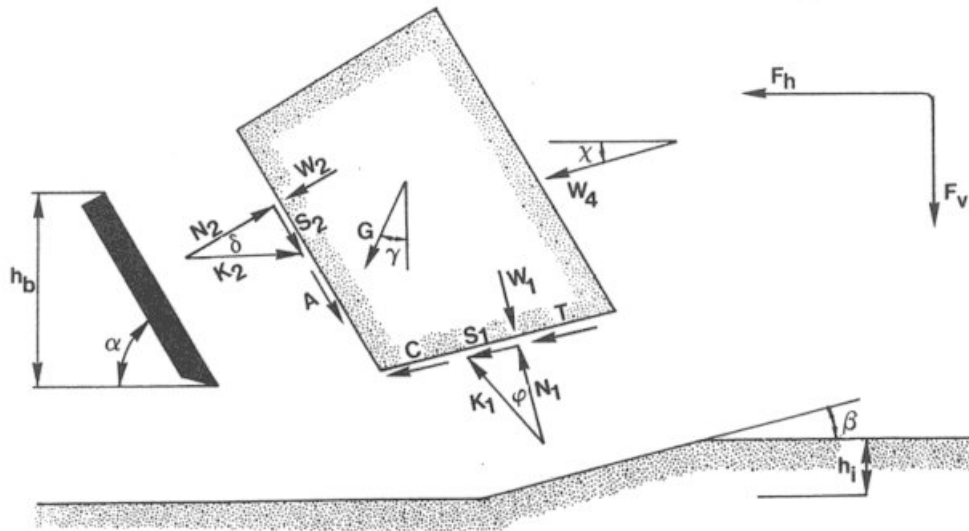


Fig. 12: The forces acting on the layer of soil cut.

The normal force N_1 and the shear force S_1 can be combined to a resulting grain force K_1 . By taking the horizontal and vertical equilibrium of forces an expression for the force K_2 on the blade can be derived.

The horizontal equilibrium of forces:

$$K_1 \cdot \sin(\beta + \phi) - W_1 \cdot \sin(\beta) + C \cdot \cos(\beta) + I \cdot \cos(\beta) - A \cdot \cos(\alpha) + W_2 \cdot \sin(\alpha) - K_2 \cdot \sin(\alpha + \delta) = 0 \quad (26)$$

The vertical equilibrium of forces:

$$\begin{aligned}
& - K_1 \cdot \cos(\beta + \phi) + W_1 \cdot \cos(\beta) + C \cdot \sin(\beta) + I \cdot \sin(\beta) + G + A \cdot \sin(\alpha) + W_2 \cdot \cos(\alpha) \\
& \qquad \qquad \qquad - K_2 \cdot \cos(\alpha + \delta) = 0
\end{aligned} \tag{27}$$

The force K_2 on the blade is now:

$$\begin{aligned}
K_2 = & \frac{W_2 \cdot \sin(\alpha + \beta + \phi) + W_1 \cdot \sin(\phi)}{\sin(\alpha + \beta + \delta + \phi)} + \\
& \frac{G \cdot \sin(\beta + \phi) + I \cdot \cos(\phi) + C \cdot \cos(\phi) - A \cdot \cos(\alpha + \beta + \phi)}{\sin(\alpha + \beta + \delta + \phi)}
\end{aligned} \tag{28}$$

From equation (28) the forces on the blade can be derived. On the blade a force component in the direction of cutting velocity F_h and a force perpendicular to this direction F_v can be distinguished.

$$F_h = -W_2 \cdot \sin(\alpha) + K_2 \cdot \sin(\alpha + \delta) + A \cdot \cos(\alpha) \tag{29}$$

$$F_v = -W_2 \cdot \cos(\alpha) + K_2 \cdot \cos(\alpha + \delta) - A \cdot \sin(\alpha) \tag{30}$$

The forces W_1 and W_2 due to water under pressure caused by dilatation dominate the cutting forces in sand as described in Miedema 1987 [4], however in clay these forces can be neglected. If the cohesive and adhesive forces are large enough then the gravitational force G and the inertial force I can also be neglected. Simplified equations can now be derived for the normal forces on the shear plane and on the blade:

The normal force on the shear plane is now:

$$N_1 = \frac{A \cdot \cos(\delta) - C \cdot \cos(\alpha + \beta + \delta)}{\sin(\alpha + \beta + \delta + \phi)} \cdot \cos(\phi) \tag{31}$$

The normal force on the blade is now:

$$N_2 = \frac{C \cdot \cos(\phi) - A \cdot \cos(\alpha + \beta + \phi)}{\sin(\alpha + \beta + \delta + \phi)} \cdot \cos(\delta) \tag{32}$$

If the equations (31) and (32) give a positive result, the normal forces are compressive forces, however it can be seen from the equations that the normal forces can become negative, the normal forces are tensile forces. It can be seen from these equations that the normal forces can become negative meaning that a tensile rupture might occur, depending on values for the adhesion and cohesion and the angles involved. The most critical direction where this might occur can be found from the Mohr circle.

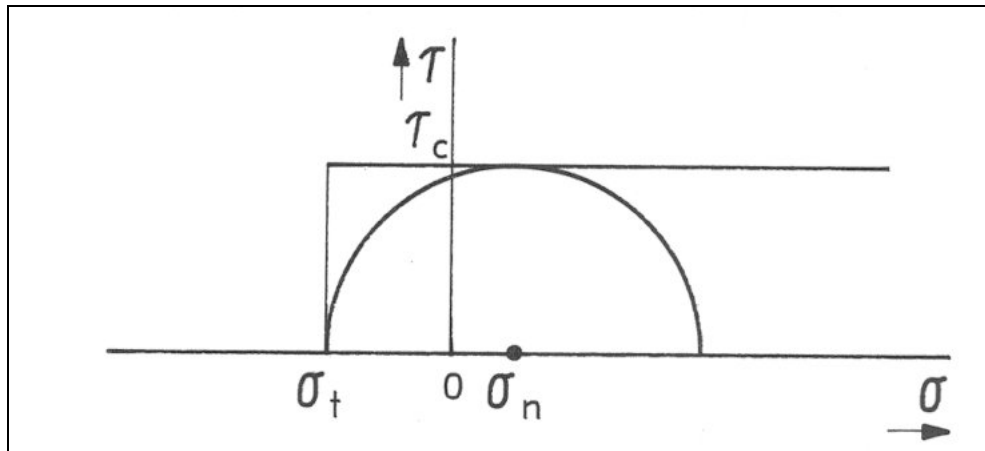


Fig. 13: The condition under which tensile failure occurs.

Figure 13 shows the Mohr circle of the conditions causing tensile rupture. It can be seen that the rupture occurs on a surface 45 degrees downwards with respect to the shearing surface. Tensile rupture will occur if:

$$\sigma_n - \tau_c = \sigma_t \quad (33)$$

If the average stresses on the shear plane are considered, this can be rewritten as an equation of forces:

$$N_1 - C = T \quad (34)$$

If a clay is considered, with an angle of internal friction and a clay/steel friction angle of zero, the following condition can be derived with respect to tensile rupture:

$$\frac{A - C \cdot \cos(\alpha + \beta)}{\sin(\alpha + \beta)} - C < T \quad (35)$$

Figure 14 shows a typical tensile rupture as noticed by Hatamura and Chijiwa 1975-1977 [2]. First a tensile rupture will occur on a plane 45 degrees downwards from the shear plane. Secondly a rupture to the free surface perpendicular with the first rupture will occur. From this condition it can be seen that the cohesive force on the shear plane is limited. The maximum cohesive force can be calculated by replacing the less than sign by the equal to sign.

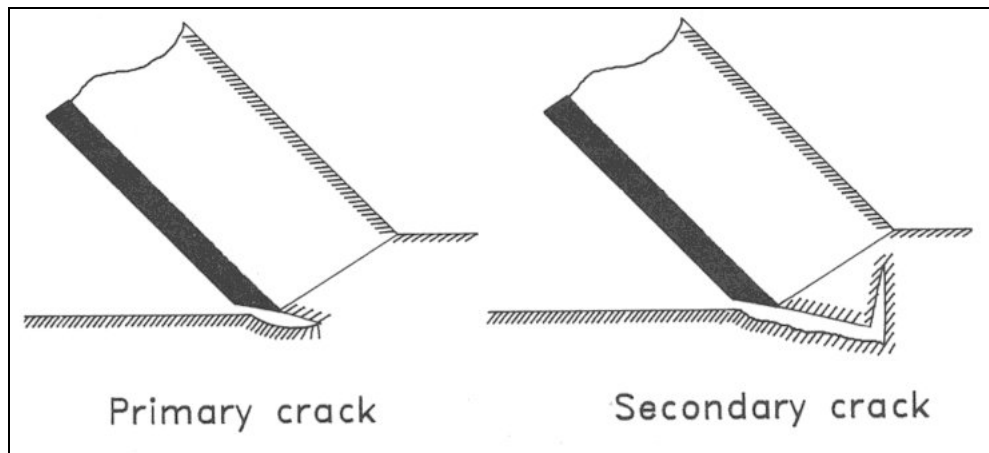


Fig. 14: Tensile rupture as described by Hatamura and Chijiwa [2].

On the blade also a critical condition may occur. The mechanism depends on the ratio between tensile strength and shear strength. If the tensile strength is greater than the shear strength, the normal force on the blade N_2 can become negative. If the tensile strength is smaller than the shear

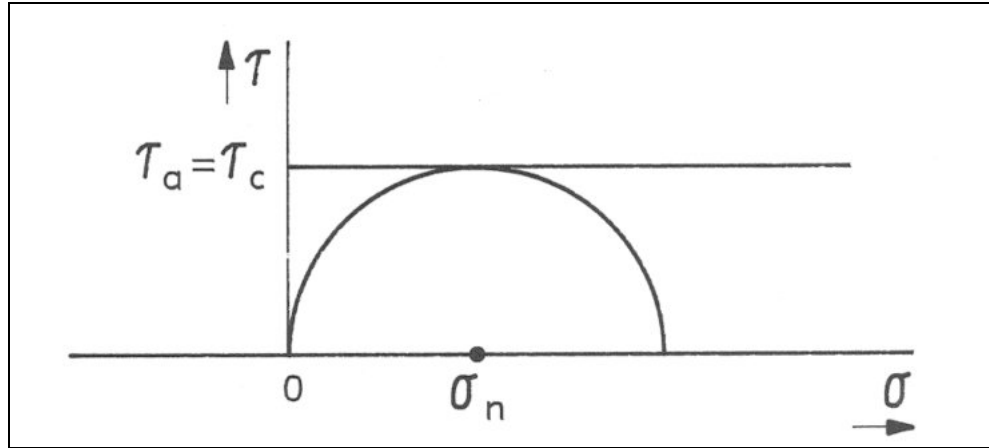


Fig. 15: The condition under which curling of the chip occurs.

strength a tensile rupture may occur under an angle upwards with respect to the blade. A more probable situation is a curling chip. Figure 15 shows the critical conditions for this case. The adhesive force is limited by this condition and can be calculated by replacing the less than sign by the equal to sign. This way also the size of the contact area between the clay and the blade can be calculated. The critical condition is:

$$\frac{C - A \cdot \cos(\alpha + \beta)}{\sin(\alpha + \beta)} - A < 0 \quad (36)$$

To interpret the conditions derived, three cases can be distinguished:

1. The condition as mentioned in equation (35) is satisfied. This may occur when cutting a very thick layer of clay. The failure mechanism will be of the "tear type".
2. Neither the conditions of equation (35) nor of equation (36) are not satisfied. This occurs when cutting a medium thick layer of clay. The failure mechanism will be of the "flow type".
3. The condition mentioned in equation (36) is satisfied. This may occur when cutting a very thin layer of clay. The failure mechanism will be of the "curling type".

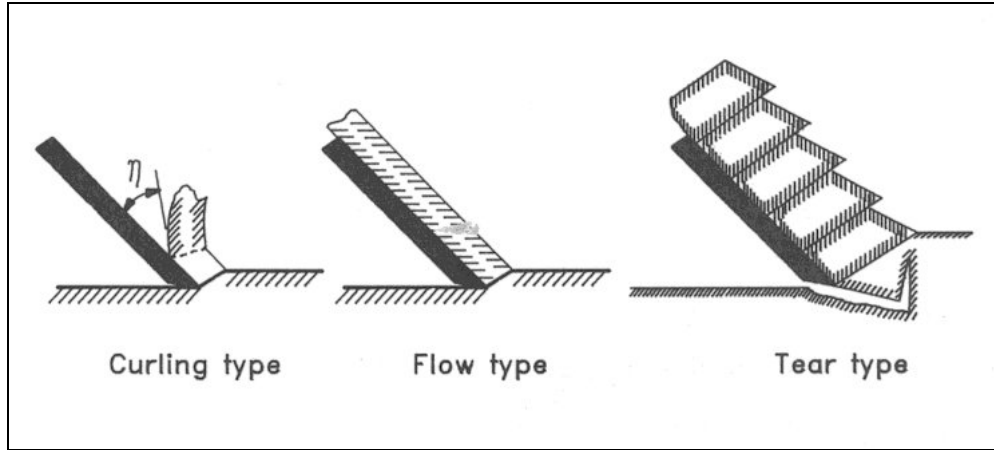


Fig. 16: The failure mechanisms.

Figure 16 shows the failure mechanisms while figure 17 gives an example of cutting forces calculated as a function of the layer thickness. Figure 18 shows cutting forces obtained by Stam [8] in relation to calculated cutting forces.

Discussion and Conclusions.

In explaining the failure mechanisms when cutting clay it is assumed that the stresses are constant over the shear plane and over the blade. It has been observed by Hatamura and Chijiwa 1975-1977 [2] that this might not be true in all cases. The method described in this paper however permits the study of the phenomena occurring during the failure of clay in a simple way. The three possible failure mechanisms can be distinguished and the most important parameters on which the occurrence of a mechanism depends are described.

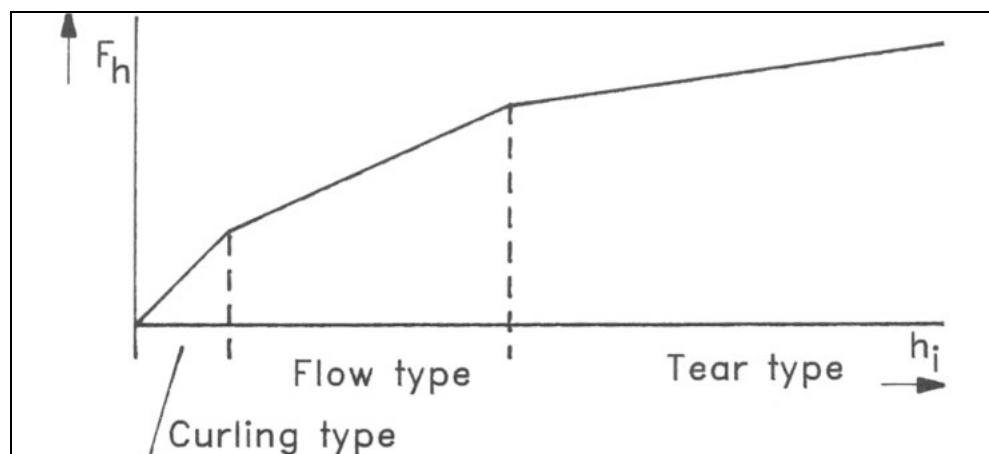


Fig. 17: The horizontal cutting force as a function of layer thickness.

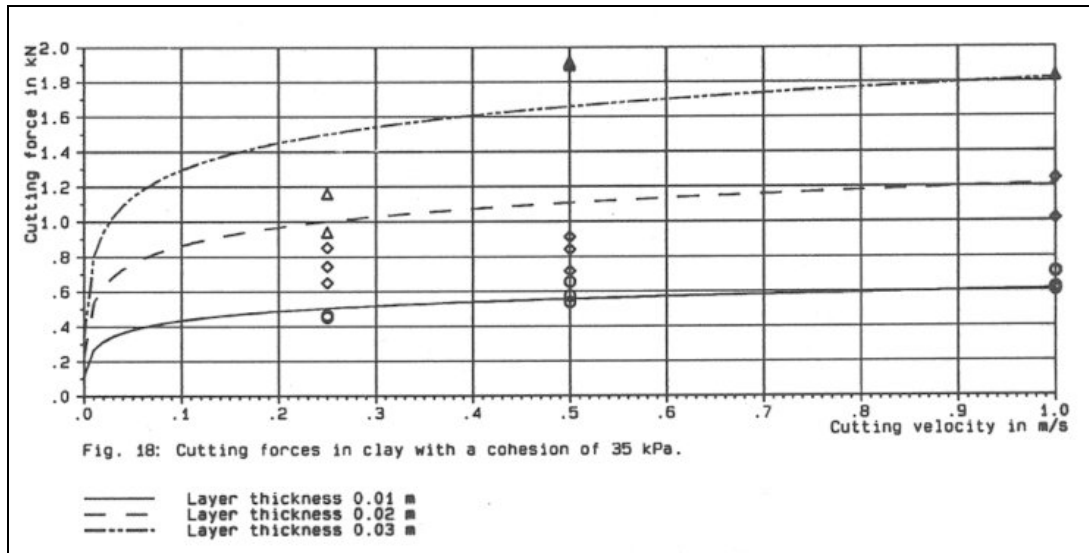


Fig. 18: The horizontal cutting force as a function of the cutting velocity (data obtained by Stam [8]).

Combining the adapted rate process theory as derived in this paper with the cutting theory allows the calculation of the cutting forces as a function of the cutting velocity. Assuming that the cohesion and the adhesion both are in accordance with equation (15) and (22) gives an explanation of the fact that the failure mechanism can change when increasing the cutting velocity while keeping all the other parameters involved constant, since the deformation rate in the shear plane will differ from the deformation rate on the blade. This implies that when the cutting velocity changes, there is a change in the ratio between the adhesive force and the cohesive force, so one of the conditions (35) or (36) may be satisfied. This has been noticed in metal cutting. The rate process theory derived is a general theory, not specific to clay. One of the advantages of this is that the rheological behaviour of silt and clay can be described by the same equation (15). Equations (23), (24) and (25) prove that equation (22) does not contradict other theories, but these equations validate the use of the theory developed.

The theory in this paper reflects some thoughts of the author in trying to solve the problem of explaining the phenomena causing yield stress. To really solve this problem, quantum mechanics should be used, but this is beyond the scope of this paper. In using the theory derived in this paper, one should understand that modelling is an attempt to describe phenomena occurring in reality without having any presumption of being reality.

Acknowledgements.

The author wishes to thank A. Klein for making some of the illustrations.

Bibliography.

1. Glasstone, S., & Laidler, K.J., & Eyring, H., "The Theory of Rate Processes". McGraw-Hill, New York, 1941.
2. Hatamura, Y, & Chijiwa, K., "Analyses of the mechanism of soil cutting".
1st report, Bulletin of the JSME, vol. 18, no. 120, June 1975.
2st report, Bulletin of the JSME, vol. 19, no. 131, May 1976.
3st report, Bulletin of the JSME, vol. 19, no. 139, November 1976.
4st report, Bulletin of the JSME, vol. 20, no. 139, January 1977.
5st report, Bulletin of the JSME, vol. 20, no. 141, March 1977.
3. Lobanov, V.A., & Joanknecht, L.W.F., "The Cutting of Soil Under Hydrostatic Pressure". Proc. WODCON IX, Vancouver, Canada, 1980.
4. Miedema, S.A., "The Calculation of the Cutting Forces when Cutting Water Saturated Sand". Doctors thesis, Delft, Holland, 1987.
5. Mitchell, J.K., "Fundamentals of Soil Behaviour". John Wiley & Sons, Inc., 1976.
6. Raalte, G.H. van & Zwartbol, A., "The Disc Bottom Cutterhead: A Report on Laboratory and Field Tests". Proc. WODCON XI, Brighton, England, 1986.
7. Soydemir, C., "Potential models for shear strength generation in soft marine clays". Int. Symp. on soft clay, Bangkok, Thailand, 5-6 june, 1977.
8. Stam, P.T., "Analyse ten behoeve van het ontwerp van een klei snijdende sleepkop". Report: CO/82/129, Delft University of Technology, 1983.
9. Turnage, G.W., and Freitag, D.R., "Effects of Cone Velocity and Size on Soil Penetration Resistance". ASEA paper 69-670, 1970.
10. Wismer, R.D., & Luth, H.J., "Rate effects in soil cutting". Journal of Terramechanics, 1972, Vol. 8, No. 3, pp. 11-21.
11. Wismer, R.D., & Luth, H.J. "Performance of Plane Soil Cutting Blades". Transactions of ASEA, 1972.
12. Zeng, D., & Yao, Y., "Investigation on the Relationship between Soil Shear Strength and Shear Rate". Journal of Terramechanics, 28(1), 1991.
13. Zeng, D., & Yao, Y., "Investigation on the Relationship Between Soil Metal Friction and Sliding Speed". Proc. of the second Asian Pacific Conf. of ISTVS, Bangkok, 1988.

Software used.

1. Miedema, S.A., "SAMWORKS", Scientific text processor, "PLOSIM", Graphical presentation of data, "CUTFORCE", Simulation of cutting processes.

List of Symbols used.

A	Adhesive force on the blade	N
B	Frequency (material property)	1/s
C	Cohesive force on shear plane	N
E	Energy level	J/kmol
E_a	Activation energy level	J/kmol
E_l	Limiting (maximum) energy level	J/kmol
f	Shear force on flow unit	N
F	Cutting force	N
G	Gravitational force	N
h	Planck constant ($6.626 \cdot 10^{-34}$ J·s)	J·s
k	Boltzman constant ($1.3807 \cdot 10^{-23}$ J/K)	J/K
K_1	Grain force on the shear plane	N
K_2	Grain force on the blade	N
i	Coefficient	-
I	Inertial force on the shear plane	N
N	Avogadro constant ($6.02 \cdot 10^{26}$ 1/kmol)	-
N_1	Normal grain force on shear plane	N
N_2	Normal grain force on blade	N
p	Probability	-
R	Universal gas constant (8314 J/kmol/K)	J/kmol/K
S	Number of bonds per unit area	1/m ²
S_1	Shear force due to internal friction on the shear surface	N
S_2	Shear force due to soil/steel friction on the blade	N
T	Absolute temperature	K
T	Tensile force	N
v	Cutting velocity	m/s
W_1	Force resulting from pore underpressure on the shear plane	N
W_2	Force resulting from pore underpressure on the blade	N

X	Function	-
α	Blade angle	rad
β	Angle of the shear plane with the direction of cutting velocity	rad
ν	frequency of activation	1/s
λ	Distance between equilibrium positions	m
$d\varepsilon/dt$	Strain rate	1/s
$d\varepsilon_0/dt$	Frequency (material property)	1/s
τ	Shear stress	N/m ²
τ_a	Adhesive shear strength (strain rate dependent)	N/m ²
τ_c	Cohesive shear strength (strain rate dependent)	N/m ²
τ_y	Shear strength (yield stress, material property)	N/m ²
τ_{ya}	Adhesive shear strength (material property)	N/m ²
τ_{yc}	Cohesive shear strength (material property)	N/m ²
τ_0	Dynamical shearing resistance factor (material property)	N/m ²
σ_e	Effective stress	N/m ²
σ_n	Normal stress	N/m ²
σ_t	Tensile strength	N/m ²
ϕ	Angle of internal friction	rad
δ	Soil/steel friction angle	rad